Desalination and Water Treatment
www.deswater.com

doi:10.5004/dwt.2017.20639

72 (2017) 394–405
April

Synthesis of copper oxide nanoparticle and photocatalytic dye degradation study using response surface methodology (RSM) and genetic algorithm (GA)

Niyaz Mohammad Mahmoodi*, Samaneh Keshavarzi, Pardis Rezaei

Department of Environmental Research, Institute for Color Science and Technology, Tehran 1668814811, Iran, Tel. +98 021 22969771, Fax +98 021 22947537, email: mahmoodi@icrc.ac.ir (N.M. Mahmoodi), samanekeshavarzi@yahoo.com (S. Keshavarzi), rezaei.pardis@yahoo.com (P. Rezaei)

ABSTRACT

The aim of our research was to study the ability of CuO nanoparticle which was synthesized for photocatalytic dye degradation of Direct Red 31 (DR31), Reactive Red 194 (RR194) and Reactive Red 120 (RR120) and to apply response surface methodology (RSM) and genetic algorithm (GA) in the optimization of the process. The characteristics of the nanoparticle were investigated by XRD, SEM and FTIR. The experiments were analyzed using response surface methodology and genetic algorithm. A Historical Data Design was used to evaluate the effects and interactions of the four significant variables: catalyst dosage, dye concentration, reaction time and salt (inorganic anion) on the photocatalytic degradation of dyes as the process response. All the experimental data showed the good agreement with the predicted results according to RSM and GA optimizations. Under the optimized conditions (catalyst dosage, 0.005 g; dye concentration, 50 mg/L; reaction time, 180 min and inorganic anion, blank) the maximal decolorization efficiencies of 78.25% , 80.08% and 70.14% were achieved for DR31, RR194 and RR120 respectively.

Keywords: Synthesis; Copper oxide nanoparticle; Photocatalytic dye degradation; Response surface methodology; Genetic algorithm

1. Introduction

Dyes are one of the main groups of organic compounds that attendance of them in water and wastewater is a serious threat for the health of humans and aquatic creatures. 1–20% of total world production of dyes release to wastewater of textile factories and unsettle ecological equilibrium. Azo dyes are the largest group of dyes and have one or more azo bonds (N=N) in their structure. Based on the number of azo bonds, azo dyes divided to monoazo, diazo, etc. classes. There are different methods for treatment of colored effluents that are categorized to adsorption, biological, physical, and chemical processes [1–11]. In spite of the fact that biological methods are simple and low cost, because of the complex structure of azo dyes they resist against biological treatment. Most of the physical and chemical methods are ineffective and non-destructive and transfer pollutants from water to another phase and in this way causing secondary pollution. Advanced oxidation processes (AOPs) are a useful technique for the degradation of organic pollutants in water treatment using strong oxidants such as hydroxyl radicals (HO·). Among advanced oxidation processes, heterogeneous photocatalysis using semiconductor metal oxides has shown attractive features and is a promising technology for water treatment due to destruction a variety of organic and inorganic contaminants [12,13]. Photocatalytic degradation process as an AOP is a clean and green technology and one of the best promising methods because of its perfect mineralization ability of pollutants, low energy consumption and lack of creating the secondary pollutant [14–21].

Copper oxide (CuO) as a semiconductor oxide because of great characteristic such as low cost, nontoxicity and high photochemical stability is a good choice as an effective heterogeneous catalyst [7,13,22]. The hydrothermal synthesis of CuO nanoparticles is generally based on a two-step process. First, cupric hydroxide ($Cu(OH)_2$) particles are formed by the reaction of a cupric salt precursor with a basic solution,

*Corresponding author.

such as sodium hydroxide (NaOH) or ammonium hydroxide. The $Cu(OH)_2$ particles are then thermally dehydrated to obtain the CuO nanoparticles [23]. In this research, CuO nanoparticle was synthesized and investigated as a photocatalyst. The characteristics of CuO were studied by using FTIR, XRD and SEM. Photocatalytic performance of CuO nanoparticles was investigated by degradation of Direct Red 31 (DR31), Reactive Red 194 (RR194) and Reactive Red 120 (RR120) dyes in the presence of hydrogen peroxide (H_2O_2) under UV light. Dye degradation was perused by using UV-vis spectrophotometer.

The dye degradation process is affected by many factors such as catalyst dosage, dye concentration, reaction time and inorganic anion. These process parameters need to be carefully optimized to increase the process efficiency. Optimization in conventional multi-factor systems is usually conducted by varying one factor at a time. Not only is it time consuming, but the interactions among variables may also be ignored that lead to low efficiency of optimization. Therefore, in this work, the response surface methodology (RSM) and genetic algorithm (GA) have been applied to determine the optimum conditions for desirable response. The RSM is a combination of mathematical and statistical techniques that can be used as an effective tool in order to design experiments and optimize different processes [24–26]. In this study, Historical Data Design under RSM was applied to import data that already exists. Historical Data design interface on the response surface methodology can be used for importing and analyzing numerical and categorical data. Thus, the main reason of using historical data design in Design-Expert software was to evaluate the previously obtained experimental results and predict dye degradation as a function of different factors affecting the process [27,28].

Genetic algorithm (GA) is a stochastic method developed by Goldberg inspired by Darwin's theory of evolution [29]. Global optimum in mathematical programming is determined by imitation of the genetic evolution process in nature. In order to optimize and investigate the problem, GA can be applied as an efficient research technique [30,31].

The objective of this study is to choose the optimum values of catalyst dosage, dye concentration, reaction time and salt (inorganic anion) on the photocatalytic degradation of dyes. A traditional technique for experimental process optimization in response surface methodology (RSM); however, recently, genetic algorithm (GA) can be considered as a new approach to the optimization problem which is most known in the numerical field. The present paper compares these two techniques in the optimization of the photocatalytic degradation of dyes.

2. Experimental

2.1. Chemicals

The dyes chosen for this study were Direct Red 31 (DR31), Reactive Red 194 (RR194) and Reactive Red 120 (RR120) obtained from Ciba and used without further purification. The chemical structure of model dyes is presented in Fig. 1. The H_2O_2 (30%), NaCl (≥ 99.5 %), Na_2SO_4 (≥ 99 %), $NaHCO_3$ (≥ 99 %), Copper sulfate pentahydrate (≥ 99 %) and sodium hydroxide (≥ 99 %) used without any change in this study were taken from Merck.

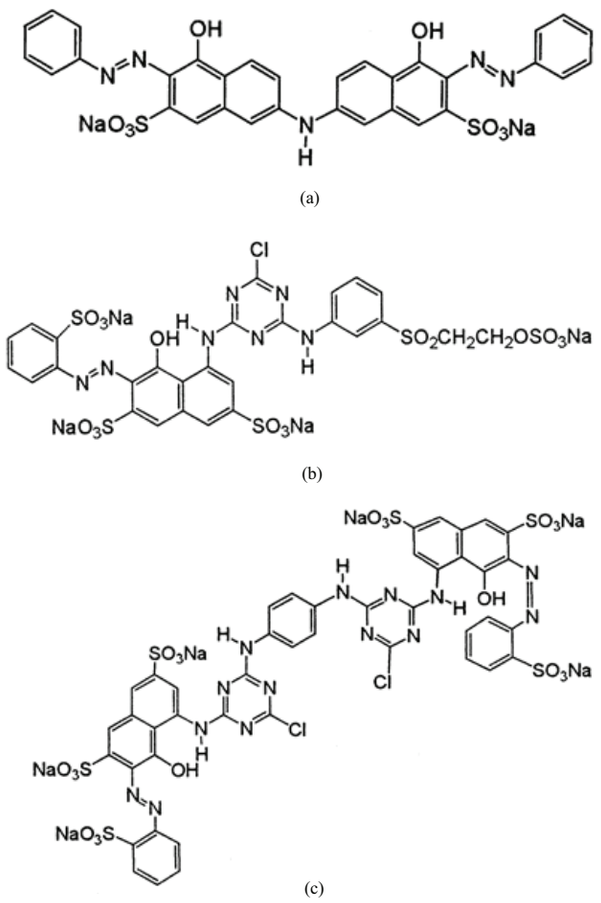

Fig. 1. The chemical structure of dyes (a) DR31, (b) RR194 and (c) RR120.

2.2. Synthesis of copper oxide nanoparticle

In 90 mL of distilled water, 1 g of $CuSO_4 \cdot 5H_2O$ and 1 g of NaOH were dissolved under stirring. The mixed solution was sealed in a glass bottle and kept static at 120°C for 24 h, and then cooled to room temperature naturally. Removing the possible residues from the final precipitate was conducted through washing with distilled water several times and then the final precipitate dried at 120°C for 12 h.

2.3. Characterization

FT-IR spectrum (Perkin-Elmer Spectrophotometer Spectrum One) was investigated. SEM (LEO 1455VP scanning microscope) was used to study the material morphology. XRD (Siemens D-5000 diffractometer with Cu Kα radiation (λ = 1.5406 A°)) was applied to indicate the material crystal structure.

2.4. Photocatalytic dye degradation

Experiments were carried out in a cylindrical batch photoreactor in volume of 1L having dimensions 14 cm height

and 5.5 cm diameter (Fig. 2). UV radiation was provided by a UV-C lamp (200–280 nm, 9 W, Philips) which was placed in the inner quartz tube and was hanged in the center of photoreactor. The effects of catalyst dosage, reaction time, initial dye concentration and presence of salt on photocatalytic dye degradation were studied in this paper.

Investigation of any effect of catalyst dosage on photocatalytic dye degradation was conducted by mixing different amounts of CuO (0–0.025 g) with 800 mL of dye solution (50 mg/L) in presence of H_2O_2 at 25°C. The samples were withdrawn at regular time intervals for 180 min. CuO was separated from the mixture by centrifuging. Then the change on the absorbance of solutions was found by UV-vis spectrophotometer at maximum wavelength of dyes (Fig. 3). The effect of initial dye concentration on photocatalytic dye degradation was determined by preparing 800 mL of solutions with different concentrations of dye (50, 75, 100 and 125 mg/L) and H_2O_2 and mixing with optimum amount of CuO (0.005 g). The effect of salt was studied and different salts including Na_2SO_4, NaCl and $NaHCO_3$ (0.01 mM) were used. The salt was mixed with 800 mL of dye solution (50 mg/L) and H_2O_2 (0.01 ml) and then the solution was contacted with 0.005 g CuO nanoparticles.

2.5. Experimental design and data analysis

Response surface methodology (RSM) is a statistical method that has a significant application in designing experiments, evaluating the effects of different factors and finding the optimum conditions as well as reducing the number of experiment [32,33]. In this study, the optimization of the four major operating variables based on the literature which were catalyst dosage (0–0.025 g), dye concentration (50–125 mg/L) and reaction time (0–180 min) as the numerical factors and salt (Blank, NaCl, $NaHCO_3$ and Na_2SO_4) as the categorical factor was calculated using Historical Data Design and RSM. The photocatalytic degradation of dyes was selected as the process response. This process was done in three systems with different dyes; DR31, RR194 and RR120.These variables and their levels are shown in Table 1.

The Design Expert Software was used to analyze experimental data. The following function was employed to calculate the coefficients of the polynomial model:

$$Y = \beta_0 + \sum_{i=1}^{n}\beta_i X_i + \sum_{i=1}^{n}\beta_{ii}X_i^2 + \sum_{i=1}^{n}\beta_{iii}X_i^3 + \sum_{i=1}^{n}\sum_{j=1}^{n}\beta_{ij}X_iX_j + \sum_{i=1}^{n}\sum_{j=1}^{n}\sum_{k=1}^{n}\beta_{ijk}X_iX_jX_k \qquad i \neq j \neq k \tag{1}$$

In this equation, Y is the response model; β_0 represents the constant coefficient; β_i, β_{ii} and β_{iii} are the linear, quadratic

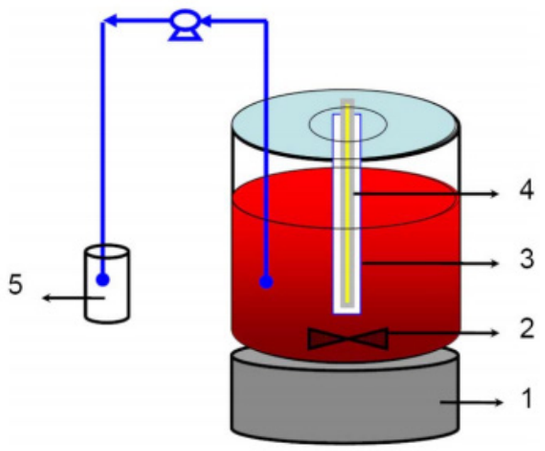

Fig. 2. Photoreactor: (1) stirrer; (2) magnet; (3) quartz tube; (4) lamp;(5) sample cell.

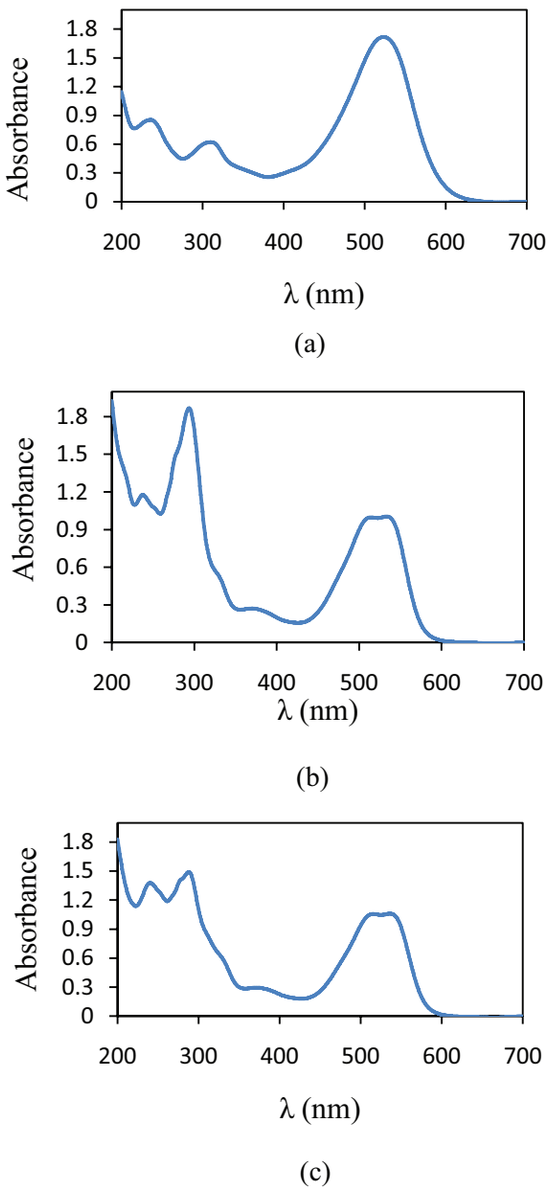

Fig. 3. UV-vis spectrum of dyes (a) DR31 (b) RR194 and (c) RR120.

Table1
Experimental range and levels of the independent variables for dyes

Dye	Variables	Type of variables	Symbol	Real value of coded levels	
				Low level(–1)	High level(+1)
DR31	Catalyst dosage (g)	Numeric	A	0	0.025
	Dye concentration (mg/L)	Numeric	B	50	125
	Reaction time(min)	Numeric	C	0	180
	Salt	Categoric	D		
RR194 and RR120	Catalyst dosage (g)	Numeric	A	0	0.015
	Dye concentration (mg/L)	Numeric	B	50	125
	Reaction time(min)	Numeric	C	0	180
	Salt	Categoric	D		

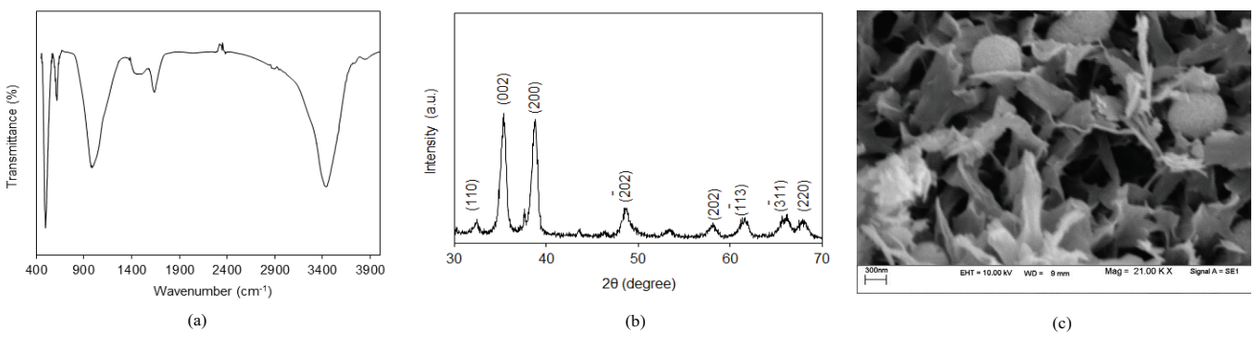

Fig. 4. The characteristics of the synthesized CuO nanoparticle (a)FT-IR spectrum, (b) XRD pattern and (c) SEM image.

and cubic coefficients respectively; β_{ij} and β_{ijk} are the interaction coefficients; n is the number of independent variables; X_i X_j, and X_k are the coded value of the independent variable.

3. Results and discussions

3.1. Characterization

Fig. 4a shows the FT-IR spectrum of CuO nanoparticle. It has two peaks at 3450 cm^{-1} and 500–600 cm^{-1} which indicate O–H stretching vibration and metal-oxygen vibration, respectively. The peak at 1625 cm^{-1} was attributed to OH bending of molecular water [34–37]. The XRD pattern of the CuO nanoparticle is presented in Fig. 4b. All diffraction peaks in Fig. 4b are in good agreement with those of the standard pattern of monoclinic CuO (JCPDS Card No. 05-0661). The Miller indices matched well with the reflections of the CuO nanoparticle reported in the previous published paper [38]. SEM is used to determine the particle shape and appropriate size distribution of the material. The SEM micrograph of the CuO nanoparticle (Fig. 4c) shows a relatively homogeneous particle size distribution.

The band gap energy of photocatalyst was calculated using $E = hc/\lambda$ relation where E= band gap energy, h = Planks constant, C = speed of light and λ = cut off wavelength. The average band gap energy of CuO nanoparticles was obtained 2.09 eV.

3.2. Model fitting and statistical analysis

Response surface methodology (Historical Data Design) was applied to analyze the relationship between the four independent variables (catalyst dosage, dye concentration, reaction time and inorganic anion) and dye degradation efficiency. Several response models such as linear, two factorial, quadratic and cubic models can be fitted to the experimental data.

The analysis of variance (ANOVA) of the regression parameters of the predicted response surface models are summarized in Table 2. Some model terms with a probability values larger than 0.05 were considered not significant and eliminated. The significance of each coefficient in equations was determined by F-value and P value. The F-values of the models are equal to 497.96, 434.09 and 311.89 for DR31, RR194 and RR120, respectively, which indicate the models are significant. There is only a 0.01% chance that the F-Value occurs due to noise. As shown in Table 2, a small probability value ($p < 0.0001$) indicates that the models were highly significant [39]. The best correlation between experimental data according to various models and their ANOVA was shown by the cubic model because of the highest coefficient of determination (R^2), adjusted R^2 and predicted R^2 values. Table 3 summarizes ANOVA results for cubic response models describing the dye degradation. The final cubic models for each response in terms of coded levels are shown in Table 4.

Table 2
ANOVA results of the cubic polynomial model for photocatalytic degradation of dyes

	Source	Sum of squares	Degree of freedom (D_f)	Mean square	F-value	P-value Prob > F	
	Model	80038.62	21	3811.36	497.96	< 0.0001	Significant
DR31	A	223.24	1	223.24	29.17	< 0.0001	
	B	14214.60	1	14214.60	1857.14	< 0.0001	
	C	54367.20	1	54367.20	7103.09	< 0.0001	
	D	4812.38	3	1604.13	209.58	< 0.0001	
	AC	21.22	1	21.22	2.77	0.0480	
	BC	3004.82	1	3004.82	392.58	< 0.0001	
	CD	352.93	3	117.64	15.37	< 0.0001	
	A2	3883.89	1	3883.89	507.43	< 0.0001	
	B2	193.87	1	193.87	25.33	< 0.0001	
	C2	2809.68	1	2809.68	367.09	< 0.0001	
	A2C	257.65	1	257.65	33.66	< 0.0001	
	BC2	182.61	1	182.61	23.86	< 0.0001	
	C2D	241.79	3	80.60	10.53	< 0.0001	
	A3	1510.24	1	1510.24	197.31	< 0.0001	
	C3	271.93	1	271.93	35.53	< 0.0001	
RR194	Model	94163.40	22	4280.15	434.09	< 0.0001	Significant
	A	424.50	1	424.50	43.05	< 0.0001	
	B	18894.17	1	18894.17	1916.24	< 0.0001	
	C	63007.04	1	63007.04	6390.14	< 0.0001	
	D	6791.09	3	2263.70	229.58	< 0.0001	
	AC	54.87	1	54.87	5.57	0.0196	
	BC	3531.31	1	3531.31	358.14	< 0.0001	
	CD	829.20	3	276.40	28.03	< 0.0001	
	A2	5064.01	1	5064.01	513.59	< 0.0001	
	B2	166.71	1	166.71	16.91	< 0.0001	
	C2	2251.11	1	2251.11	228.31	< 0.0001	
	A2C	198.61	1	198.61	20.14	< 0.0001	
	B2C	41.36	1	41.36	4.19	0.0423	
	BC2	589.13	1	589.13	59.75	< 0.0001	
	C2D	342.41	3	114.14	11.58	< 0.0001	
	A3	403.67	1	403.67	40.94	< 0.0001	
	C3	124.17	1	124.17	12.59	0.0005	
RR120	Model	70536.69	17	4149.22	311.89	< 0.0001	Significant
	A	118.15	1	118.1	8.88	0.0034	
	B	12371.18	1	12371.18	929.91	< 0.0001	
	C	46404.45	1	46404.45	3488.09	< 0.0001	
	D	2910.45	1	970.15	72.92	< 0.0001	
	AC	33.23	1	33.23	2.50	0.0418	
	BC	1484.02	1	1484.02	111.55	< 0.0001	
	CD	120.77	3	40.26	3.03	0.0314	
	A2	4949.24	1	4949.24	372.02	< 0.0001	
	B2	53.97	1	53.97	4.06	< 0.0001	
	C2	2631.22	1	2631.22	197.78	< 0.0001	
	A2C	605.68	1	605.68	45.53	< 0.0001	
	BC2	315.43	1	315.43	23.71	< 0.0001	
	A3	6837.81	1	6837.81	513.98	< 0.0001	

3.3. Effect of the variables studied

The effect of CuO dosage and reaction time on the photocatalytic degradation of dyes at a fixed dye concentration of 50 mg/L is shown in Fig. 5. As can be seen, increasing the dosage of catalyst up to 0.005 g can enhance the percentage of decolorization and then it is followed by a gradual decrease in dye degradation with increasing catalyst dosage. A possible explanation for this behavior can be the turbidity of the solution in high amount of catalyst [10,15]. Therefore dyes degradations in the optimum dosage of catalyst (0.005 g) are 78.25%, 80.08% and 70.14% for DR31, RR194 and RR120, respectively.

Fig. 6 illustrates the effect of initial dye concentration and reaction time on the photocatalytic degradation of dyes in a CuO dosage of 0.005 g. The results indicate that initial dye concentration has an inverse effect on the degradation efficiency. This negative impact has two main reasons as follows: as dye concentration in solution increase, it acts like a filter and prevents from achieving of light to the surface of photocatalyst. In addition to this, more molecules of dye are absorbed on the surface of photocatalyst by increasing in dye concentration and thus the number of active sites for producing hydroxyl radicals reduces [7,10,14,15].

Presence of salts in wastewater of textile industries is an ineluctable reality. As shown in Fig. 7, presence of salt reduces the dye degradation efficiency. Salts reduce the performance of dye degradation by reacting with hydroxyl radicals and inactivation the active sites.

It is clear that bicarbonate land to more deduction in effectiveness of dye degradation toward the other ions, chloride and sulfate. Because apart from reacting with hydroxyl radicals, bicarbonate prevent from producing of hydroxyl radicals dye decomposition of hydrogen peroxide [14].

Table 3
ANOVA results for response models

Dye	R-squared	Adjusted R-squared	Predicted R-squared
DR31	0.9864	0.9841	0.9815
RR194	0.9852	0.9827	0.9800
RR120	0.9749	0.9707	0.9627

3.4. Kinetic reaction and mechanism of photocatalytic dye degradation

Decolorization kinetic was surveyed at different catalyst dosages. The curves were fitted using zero-order, first-order and second-order models,according to the noble expressions:

Table 4
Cubic models for each response in terms of coded levels for dyes

Dye	Salt	Decolorization, %=
DR31	Blank	+29.04–25.08A–20.30B+18.81C–0.54AC–11.38BC–15.80A2+3.92B2–14.25C2 –7.81A2 C+5.19BC2+27.57A3+6.83C3
	NaCl	+30.98–25.08A–20.30B+20.79C–0.54 AC–11.38BC–15.80A2+3.92B2–13.95C2 –7.81A2 C+5.19BC2+27.57A3+6.83C3
	Na_2SO_4	+2.24–25.08 A–20.30B+11.22C –0.54AC–11.38BC –15.80A2+3.92B2+2.81C2 –7.81A2 C+5.19BC2+27.57A3+6.83C3
	$NaHCO_3$	+17.96–25.08A–20.30B+19.46C–0.54 AC–11.38BC–15.80A2+3.92B2–5.64C2 –7.81A2 C+5.19BC2 +27.57A3+6.83C3
RR194	Blank	+31.29–4.57A–24.76B+19.15C+2.26AC –12.05 BC–18.68A2+4.07B2–6.26C2 –5.98 A2 C+2.84B2 C+9.33BC2+2.84B2 C +11.14A3+4.62C3
	NaCl	+23.55–4.57A–24.76B+20.72C+2.26AC–12.05 BC–18.68A2+4.07B2–2.19C2 –5.98A2 C +9.33BC2+2.84B2 C+11.14A3+4.62C3
	Na_2SO_4	–2.05–4.57A–24.76B+6.46C+2.26AC–12.05BC–18.68A2+4.07B2+8.54C2 –5.98A2 C+2.84B2 C+9.33BC2+11.14A3+4.62C3
	$NaHCO_3$	+16.37–4.57A–24.76B+19.02C+2.26AC–12.05BC–18.68A2+4.07B2+2.03C2 –5.98 A2 C+2.84B2 C+9.33BC2 +11.14A3+4.62C3
RR120	Blank	+22.08–39.37A–19.52B+23.23C–0.88AC–8.19BC–14.51A2+2.07B2–7.21C2 –10.37A2 C+6.57BC2+46.00 A3
	NaCl	+18.93–39.37A–19.52B+23.63 C–0.88 AC–8.19BC–14.51A2+2.07B2–7.21C2 –10.37A2 C+6.57BC2+46.00A3
	Na_2SO_4	+11.97–39.37A–19.52B+20.9C–0.88AC–8.19BC–14.51A2+2.07B2–7.21C2 –10.37A2 C+6.57BC2+46.00A3
	$NaHCO_3$	+5.78–39.37A–19.52B+18.36C–0.88AC–8.19BC–14.51A2+2.07B2–7.21C2 –10.37A2 C+6.57BC2+46.00A3

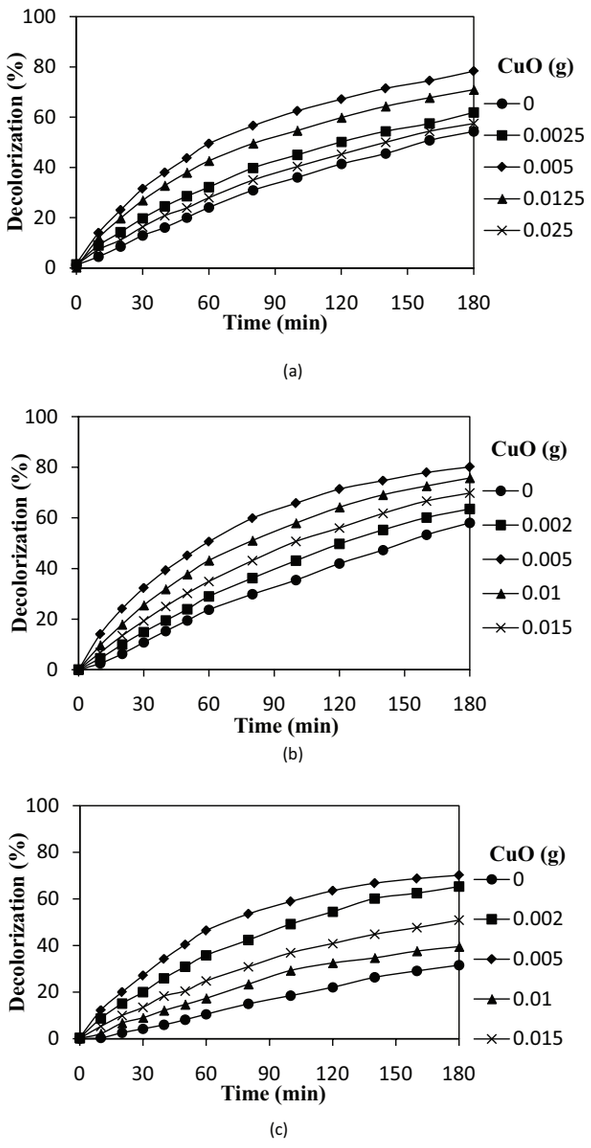

Fig. 5. The effect of CuO dosage on the photocatalytic degradation of dyes using UV/CuO/H_2O_2 (a) DR31, (b) RR194 and (c) RR120.

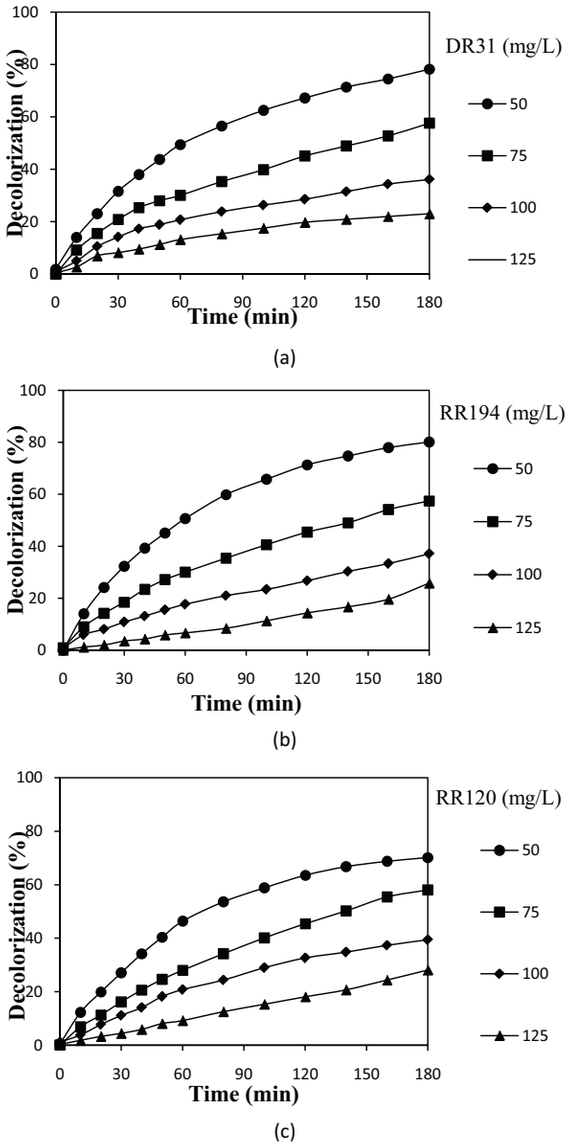

Fig. 6. The effect of dye concentration on the photocatalytic degradation of dyes using UV/CuO /H_2O_2 (a) DR31, (b) RR194 and (c) RR120.

$$C - C_0 = -k_0 t \quad (2)$$

$$C/C_0 = \exp(-k_1 t) \quad (3)$$

$$(1/C) - (1/C_0) = k_2 t \quad (4)$$

where C_0 = initial dye concentration (mg/L), C = dye concentration at time t (mg/L), k_0 = zero-order rate constant (mg/min L), k_1 = first-order rate constant (l/min) and k_2 = second-order rate constant (L/mg min).

The decolorization kinetics constants are presented in Table 5. According to the results, it is clear that the dye degradation kinetics followed first-order kinetic model and indicate that photocatalytic dye degradation depends on catalyst dosage.

Radiation of light with sufficient energy to overcome the band gap energy of photocatalyst excites electrons and makes them to migrate to the conduction band of photocatalyst. In addition, this migration creates some holes in valance band. These electrons and holes produce some oxidizing agents like hydroxyl radicals by participating in redox reactions. Hydroxyl radical is a non-selective and rapid oxidant and is the main agent of dye degradation. Photogenerated electron-hole pairs tend to recombine together and release the stored energy immediately. But presence of electron scavengers like molecular oxygen and hydrogen peroxide prevents merging and allows the continuation of reactions. Mechanism of photocatalytic degradation of dyes is as follows [10]:

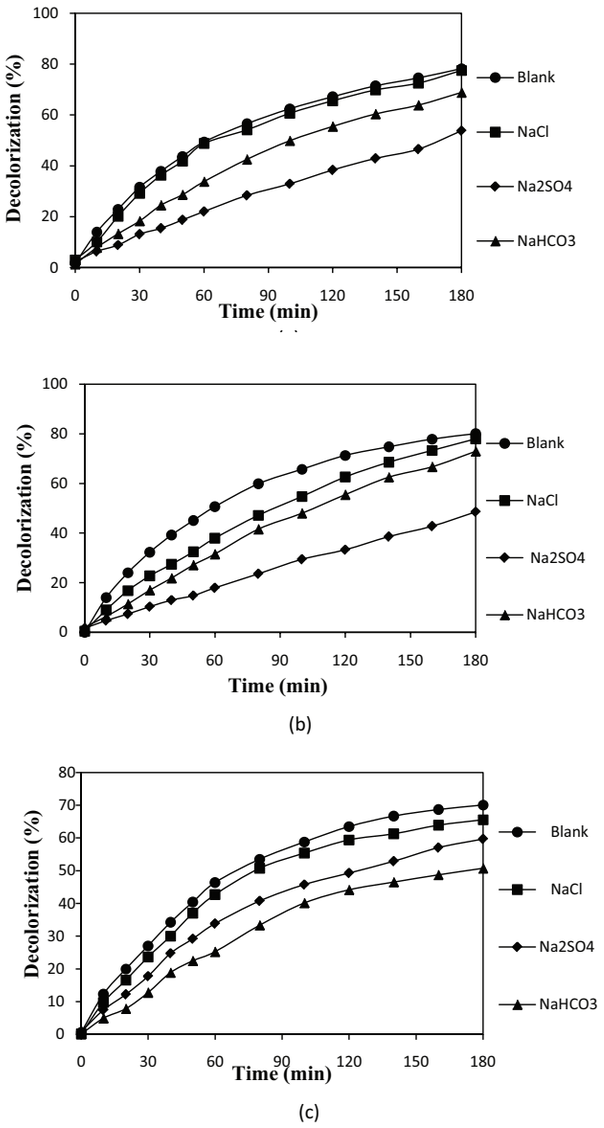

Fig. 7. The effect of salt (inorganic anion) on the photocatalytic degradation of dyes using UV/CuO/H_2O_2 (a) DR31, (b) RR194 and (c) RR120.

$$\text{Photocatalyst} + h\nu \rightarrow \text{photocatalyst}\ (e_{CB}^- + h_{VB}^+) \quad (5)$$

$$h_{VB}^+ + H_2O \rightarrow H^+ + OH\cdot \quad (6)$$

$$h_{VB}^+ + OH^- \rightarrow OH\cdot \quad (7)$$

$$e_{CB}^- + O_2 \rightarrow O_2\cdot^- \quad (8)$$

$$O_2\cdot^- + H^+ \rightarrow HO_2\cdot \quad (9)$$

$$2\,HO_2\cdot \rightarrow H_2O_2 + O_2 \quad (10)$$

$$e_{CB}^- + H_2O_2 \rightarrow OH\cdot + OH^- \quad (11)$$

$$H_2O_2 + h\nu \rightarrow 2OH\cdot \quad (12)$$

$$\text{Dye} + OH\cdot \rightarrow \text{degradation products} \quad (13)$$

$$\text{Dye} + h_{VB}^+ \rightarrow \text{oxidation products} \quad (14)$$

$$\text{Dye} + e_{CB}^- \rightarrow \text{reduction products} \quad (15)$$

3.5. Optimization conditions and verification

The response models derived from experimental data were used to determine the optimal conditions for maximum degradation of dyes. In RSM, the desired goal for each variables and response can be set. In the present study, the desired goals are defined maximum process degradation while the process variables A, B and C were selected to be in range. Table 6 presents the results.

GA, MATLAB optimization toolbox, is an optimization technique applied to the cubic equations for the photocatalytic degradation of dyes. The dye degradation optimization in GA was done by defining:

Variables: catalyst dosage (A), dye concentration (B) and reaction time (C)

Variable range: $-1 \leq A \leq +1$, $-1 \leq B \leq +1$ and $-1 \leq C \leq +1$

Maximize degradation process = f (A, B and C)

Degradation process ≤ 100%

where –1 and +1 are the low level and high level of variables in the cubic model equations (Table 4).

Table 7 shows the optimum variables and response. The optimum coded variables in GA optimization for the photocatalytic degradation of dyes are presented in Figs. 8, 9 and 10.

As we can see, optimization by RSM and GA demonstrated that the experimental results (Table 8) were close to the results obtained by optimization methods.

Additional experiments were then conducted to confirm the optimum results and each experiment is repeated for three rimes. Table 9 shows dye degradation from laboratory experiments that agree with the predicted values from RSM and GA optimization.

4. Conclusion

In this study, copper oxide nanoparticle was synthesized, characterized and employed in photocatalytic degradation of Direct Red 31 (DR31), Reactive Red 194 (RR194) and Reactive Red 120 (RR120) in presence of H_2O_2. The effect of four significant process variables including catalyst dosage, dye concentration, reaction time and salt on dye degradation was studied. Response surface methodology and genetic algorithm were applied to optimize the photocatalytic dye degradation. This study showed that response surface methodology and genetic algorithm were the suitable optimization methods in order to maximize the photocatalytic degradation of DR31, RR194 and RR120 at optimum conditions. The good agreement between RSM and GA optimi-

Table 5
The decolorization kinetics constants (R^2 = correlation coefficient)

Dye	Catalyst (g)	Zero-order		First-order		Second-order	
		k_0	R^2	k_1	R^2	k_2	R^2
DR31	0.000	0.0054	0.979	0.0043	0.9991	0.0035	0.9817
	0.002	0.0075	0.8977	0.0056	0.995	0.0044	0.985
	0.005	0.009	0.7474	0.009	0.9839	0.0104	0.9696
	0.010	0.0088	0.7751	0.0075	0.9955	0.007	0.9622
	0.015	0.0062	0.9441	0.0049	0.9953	0.004	0.9916
RR194	0.000	0.0034	0.9907	0.0046	0.9946	0.0066	0.9551
	0.002	0.0039	0.9682	0.0057	0.9993	0.0087	0.9678
	0.005	0.0058	0.7179	0.0099	0.9844	0.0203	0.968
	0.010	0.0052	0.8487	0.0083	0.9904	0.0153	0.9745
	0.015	0.0045	0.9281	0.0069	0.9985	0.0114	0.9692
RR120	0.000	0.0018	0.9936	0.0021	0.9892	0.0024	0.9781
	0.002	0.0047	0.8834	0.0064	0.9926	0.0093	0.9838
	0.005	0.0054	0.7271	0.0078	0.9949	0.0125	0.9297
	0.010	0.0027	0.9614	0.003	0.9931	0.0035	0.9851
	0.015	0.0036	.09356	0.0042	0.9986	0.0051	0.9868

Table 6
Optimal conditions of the photocatalytic degradation of dyes according to RSM

Dye	A (g)	B (mg/L)	C (min)	D	Decolorization (%)	Desirability factor
DR31	0.0081	50.16	178.04	Blank	80.3881	1.000
	0.0085	51.73	180.00	NaCl	78.3505	1.000
	0.0082	50.00	180.00	Na_2SO_4	58.5854	0.749
	0.0082	50.00	180.00	$NaHCO_3$	73.9292	0.945
RR194	0.0072	51.93	179.70	Blank	80.5775	1.000
	0.0072	50.78	179.72	NaCl	80.2025	1.000
	0.0072	50.00	180.00	Na_2SO_4	52.0102	0.649
	0.0072	50.00	180.00	$NaHCO_3$	76.4902	0.955
RR120	0.0044	50.03	179.32	Blank	70.4151	1.000
	0.0046	50.00	180.00	NaCl	67.7462	0.966
	0.0046	50.00	180.00	Na_2SO_4	58.0651	0.828
	0.0046	50.00	172.67	$NaHCo_3$	49.4156	0.704

Table 7
Optimal conditions of the photocatalytic degradation of dyes according to GA

	A		B		C		D	Decolorization (%)
	Coded	Real(g)	Coded	Real(mg/L)	Coded	Real(min)		
DR31	–0.3385	0.0083	–1.0000	50	1.0000	180	Blank	81.0061
	–0.3400	0.0083	–1.0000	50	1.0000	180	NaCl	79.9578
	–0.3978	0.0075	–1.0000	50	1.0000	180	Na_2SO_4	59.4209
	–0.3400	0.0083	–1.0000	50	1.0000	180	$NaHCo_3$	73.8833
RR194	–0.0456	0.0072	–1.0000	50	1.0000	180	Blank	80.4015
	–0.0452	0.0072	–1.0000	50	1.0000	180	NaCl	81.0730
	–0.0456	0.0072	–1.0000	50	1.0000	180	Na_2SO_4	52.0129
	–0.0454	0.0072	–1.0000	50	1.0000	180	$NaHCo_3$	76.4711
RR120	–0.3894	0.0046	–1.0000	50	1.0000	180	Blank	70.4814
	–0.3896	0.0046	–1.0000	50	1.0000	180	NaCl	67.7432
	–0.3892	0.0046	–1.0000	50	1.0000	180	Na_2SO_4	58.0490
	–0.3894	0.0046	–1.0000	50	1.0000	180	$NaHCo_3$	49.4165

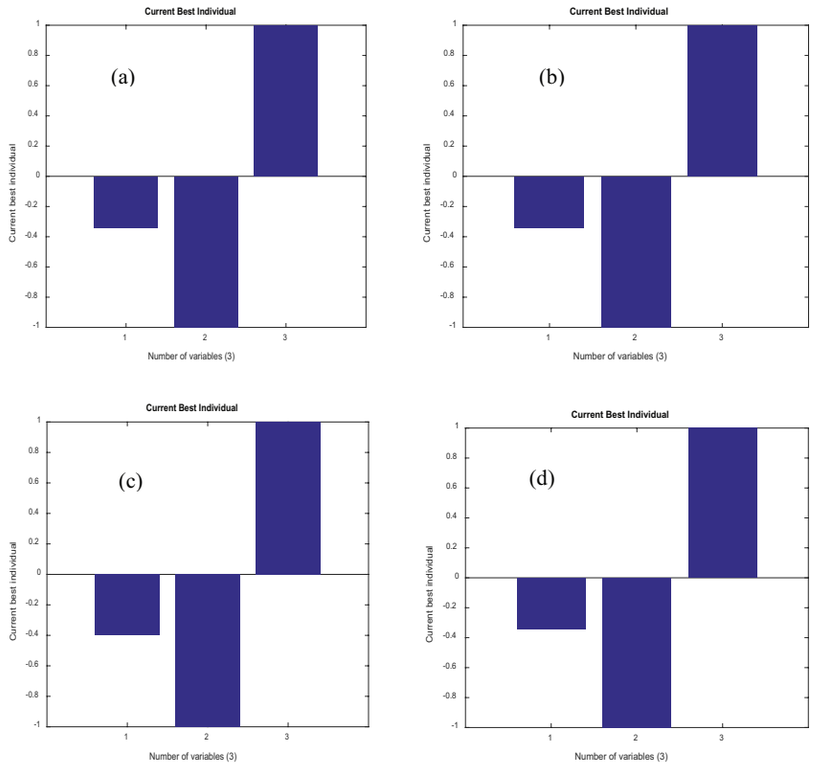

Fig. 8. Plots of current best individuals *vs.* number of variables in GA Optimization for the photocatalytic degradation of DR31: (a) Blank, (b) NaCl, (c) Na_2SO_4 and (d) $NaHCO_3$.

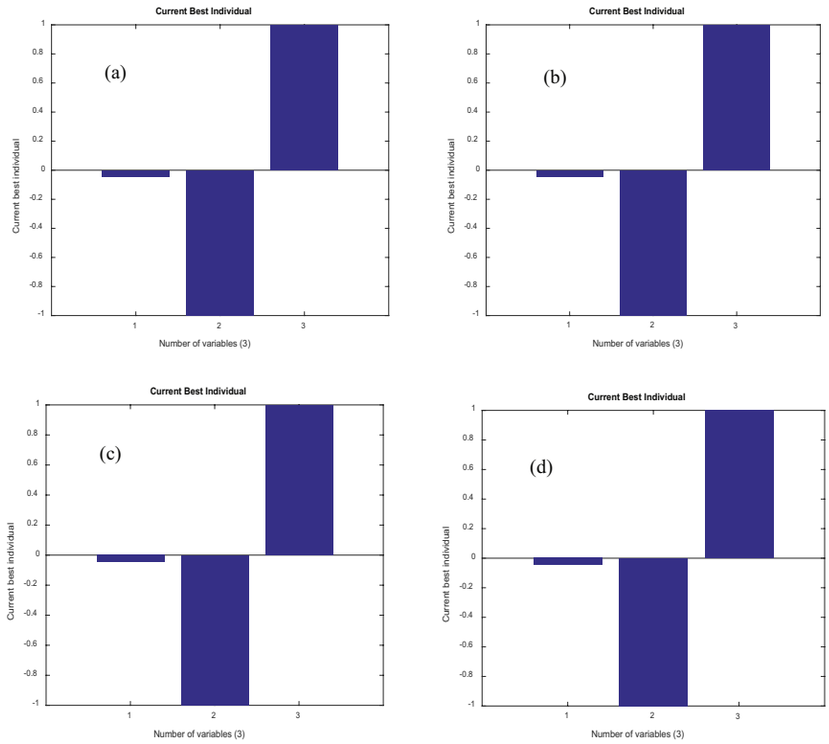

Fig. 9. Plots of current best individuals *vs.* number of variables in GA Optimization for the photocatalytic degradation of RR194: (a) Blank, (b) NaCl, (c) Na_2SO_4 and (d) $NaHCO_3$.

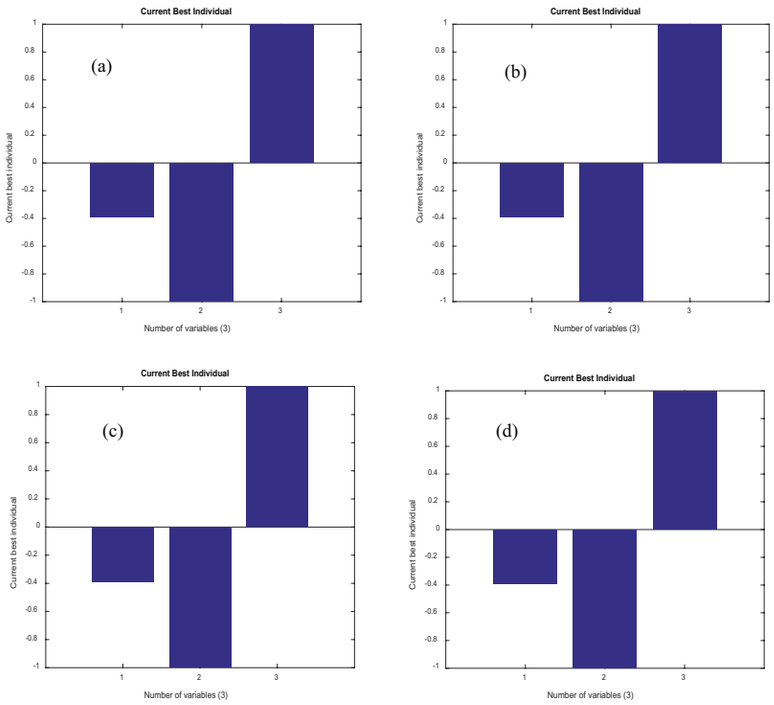

Fig. 10. Plots of current best individuals *vs.* number of variables in GA Optimization for the photocatalytic degradation of RR120: (a) Blank, (b) NaCl, (c) Na_2SO_4 and (d)$NaHCO_3$.

Table 8
Optimal conditions of the photocatalytic degradation of dyes according to experimental study

Dye	A (g)	B (mg/L)	C (min)	D	Decolorization (%)
DR31	0.005	50.00	180.00	Blank	78.25
RR194	0.005	50.00	180.00	Blank	80.08
RR120	0.005	50.00	180.00	Blank	70.14

Table 9
Comparison between obtained and predicted values according to RSM and GA.

Dye	A (g)	B (mg/L)	C (min)	D	Decolorization (%)		
					RSM	GA	Experimental
DR31	0.008	50.00	180.00	Blank	80.3881	81.0061	77.68
RR194	0.007	50.00	180.00	Blank	80.5775	80.4015	79.24
RR120	0.0046	50.00	180.00	Blank	70.4151	70.4814	70.08

zation results and experimental data confirmed the models adequacy. The results indicate that both methods are capable of determining optimum conditions. The optimum values of catalyst dosage, dye concentration, reaction time and salt were 0.005 g, 50 mg/L, 180 min and blank, respectively.

References

[1] N.M. Mahmoodi, Manganese ferrite nanoparticle: Synthesis, characterization and photocatalytic dye degradation ability, Desal. Water Treat., 53 (2015) 84–90.

[2] N.M. Mahmoodi, Surface modification of magnetic nanoparticle and dye removal from ternary systems, J. Ind. Eng. Chem., 27 (2015) 251–259.

[3] N.M. Mahmoodi, F. Najafi, Synthesis, amine functionalization and dye removal ability of titania/silica nano-hybrid, Micropor. Mesopor. Mater., 156 (2012) 153–160.

[4] N.M. Mahmoodi, Dendrimer functionalized nanoarchitecture: Synthesis and binary system dye removal. J. Taiwan Inst. Chem. Eng., 45 (2014) 2008–2020.

[5] N.M. Mahmoodi, Synthesis of core-shell magnetic adsorbent nanoparticle and selectivity analysis for binary system dye removal, J. Ind. Eng. Chem., 20 (2014) 2050–2058.

[6] N.M. Mahmoodi, Nickel ferrite nanoparticle: synthesis, modification by surfactant and dye removal ability, Water, Air, Soil Pollution, 224 (2013) 1419.
[7] K. Mageshwari, R. Sathyamoorthy, J. Park, Photocatalytic activity of hierarchical CuO microspheres synthesized by facile reflux condensation method, Powder Technol., 278 (2015) 150–156.
[8] N.M. Mahmoodi, Synthesis of amine functionalized magnetic ferrite nanoparticle and its dye removal ability, J. Environ. Eng., 139 (2013) 1382–1390.
[9] N.M. Mahmoodi, B. Hayati, M. Arami, Kinetic, equilibrium and thermodynamic studies of ternary system dye removal using a biopolymer, Ind. Crops Prod., 35 (2012) 295–301.
[10] I.K. Konstantinou, T.A. Albanis, TiO_2-assisted photocatalytic degradation of azo dyes in aqueous solution: kinetic and mechanistic investigations: a review, Appl. Catal. B: Environ., 49 (2004) 1–14.
[11] N.M. Mahmoodi, B. Hayati, M. Arami, F. Mazaheri, Single and binary system dye removal from colored textile wastewater by a dendrimer as a polymeric nanoarchitecture: equilibrium and kinetics, J. Chem. Eng. Data, 55 (2010) 4660–4668
[12] N.M. Mahmoodi, Photodegradation of dyes using multiwalled carbon nanotube and ferrous ion, J. Environ. Eng., 139 (2013) 1368–1374.
[13] K. Mageshwari, D. Nataraj, T. Pal, R. Sathyamoorthy, J. Park, Improved photocatalytic activity of ZnO coupled CuO nanocomposites synthesized by reflux condensation method, J. Alloys Compd., 625 (2015) 362–370.
[14] N.M. Mahmoodi, Synthesis of magnetic carbon nanotube and photocatalytic dye degradation ability, Environ. Monit.Assess., 186 (2014) 5595–5604.
[15] N.M. Mahmoodi, Binary catalyst system dye degradation using photocatalysis, Fibers Polym., 15 (2014) 273–280.
[16] D. Sudha, P. Sivakumar, Review on the photocatalytic activity of various composite catalysts, Chem. Eng. Proc: Proc. Inten., 97 (2015) 112–133.
[17] N.M. Mahmoodi, Photocatalytic ozonation of dyes using multiwalled carbon nanotube, J. Mole. Catal. A: Chem., 366 (2013) 254–260.
[18] N.M. Mahmoodi, Photocatalytic degradation of dyes using carbon nanotube and titania nanoparticle, Water, Air, Soil Pollution, 224 (2013) 1612.
[19] S. Kaur, S. Sharma, S.K. Kansal, Synthesis of ZnS/CQDs nanocomposite and its application as a photocatalyst for the degradation of an anionic dye, ARS. Superlat. Microstructures, 98 (2016) 86–95.
[20] S. Kumar, S. Sharma, A. Umar, S.K. Kansal, Bismuth sulphide (Bi_2S_3) nanotubes as an efficient photocatalyst for methylene blue dye degradation, Nanosci. Nanotechnol. Let., 8 (2016) 266–272.
[21] S. Kumar, S. Sharma, S. Sood, A. Umar, S.K. Kansal, Bismuth sulfide (Bi_2S_3) nanotubes decorated TiO_2 nanoparticles heterojunction assembly for enhanced solar light driven photocatalytic activity, Ceram. Inter., 42 (2016) 17551–17557.
[22] S. Sonia, S. Poongodi, P.S. Kumar, D. Mangalaraj, N. Ponpandian, C. Viswanathan, Hydrothermal synthesis of highly stable CuO nanostructures for efficient photocatalytic degradation of organic dyes, Mater. Sci. Semicond. Processing, 30 (2015) 585–591.
[23] Q. Zhang, K. Zhang, D. Xu, G. Yang, H. Huang, F. Nie, C. Liu, S. Yang, CuO nanostructures: Synthesis, characterization, growth mechanisms, fundamental properties, and applications, Prog. Mater. Sci., 60 (2014) 208–337.
[24] G.E. Box, N.R. Draper, Empirical Model-Building and Response Surfaces. Vol. 424. 1987: Wiley New York.
[25] W.J. Hill, W.G. Hunter, A review of response surface methodology: a literature survey, Technometrics, 8 (1966) 571–590.
[26] I.H. Cho, K.D. Zoh, Photocatalytic degradation of azo dye (Reactive Red 120) in TiO_2/UV system: optimization and modeling using a response surface methodology (RSM) based on the central composite design, Dyes Pigments, 75 (2007) 533–543.
[27] Z. Jeirani, B.M. Jan, B.S. Ali, I.M. Noor, C.H. See, W. Saphanuchart, Prediction of the optimum aqueous phase composition of a triglyceride microemulsion using response surface methodology, J. Ind. Eng. Chem., 19 (2013) 1304–1309.
[28] K. Charoen, C. Prapainainar, P. Sureeyatanapas, T. Suwannaphisit, K. Wongamornpitak, P. Kongkachuichay, S.M. Holmes, Application of response surface methodology to optimize direct alcohol fuel cell power density for greener energy production, J. Clean. Prod., 142 (2017) 1309–1320.
[29] D.E. Goldberg, Genetic Algorithms in Search, Optimization, and Machine Learning, Addison-Wesley Longman Publishing Co., Inc. Boston, MA, USA, 1989.
[30] Z. Michalewicz, M. Schoenauer, Evolutionary algorithms for constrained parameter optimization problems, Evolut. Comput., 4 (1996) 1–32.
[31] A.S. Dawood, Y. Li, Modeling and optimization of new flocculant dosage and pH for flocculation: removal of pollutants from wastewater, Water, 5 (2013) 342–355.
[32] D. Baş, İ.H. Boyacı, Modeling and optimization I: Usability of response surface methodology, J. Food Eng., 78 (2007) 836–845.
[33] R.L. Mason, R.F. Gunst, J.L. Hess, Statistical Design and Analysis of Experiments: With Applications to Engineering and Science, John Wiley & Sons, Inc., Hoboken, New Jersey, 2003.
[34] S. Muthulingam, I.-H. Lee, P. Uthirakumar, Highly efficient degradation of dyes by carbon quantum dots/N-doped zinc oxide (CQD/N-ZnO) photocatalyst and its compatibility on three different commercial dyes under daylight, J. Colloid Interface Sci., 455 (2015) 101–109.
[35] S. Maensiri, C. Masingboon, B. Boonchom, S. Seraphin, A simple route to synthesize nickel ferrite ($NiFe_2O_4$) nanoparticles using egg white, Scripta Materialia, 56 (2007) 797–800.
[36] M. Mouallem-Bahout, S. Bertrand, O. Peña, Synthesis and characterization of Zn 1– $xNixFe_2O_4$ spinels prepared by a citrate precursor, J. Solid State Chem., 178 (2005) 1080–1086.
[37] D.L. Pavia, G.M. Lampman, G.S. Kaiz, Introduction to Spectroscopy: A Guide for Students of Organic Chemistry, W.B Saunders Company, New York, NY, 1987.
[38] B. Li, Y. Wang, Facile synthesis and photocatalytic activity of ZnO–CuO nanocomposite, Superlat. Microstructures, 47 (2010) 615–623.
[39] E. Bayraktar, Response surface optimization of the separation of DL-tryptophan using an emulsion liquid membrane, Process Biochem., 37 (2001) 169–175.